Sensitivity of complete bandgaps to the shift of movable dielectric rod in two-dimensional photonic crystals with complex lattices

2004 J. Phys.: Condens. Matter 16 4557

(http://iopscience.iop.org/0953-8984/16/25/013)

INSTITUTE OF PHYSICS PUBLISHING JOURNAL OF PHYSICS: CONDENSED MATTER

J. Phys.: Condens. Matter **16** (2004) 4557–4566 PII: S0953-8984(04)76732-6

Sensitivity of complete bandgaps to the shift of movable dielectric rod in two-dimensional photonic crystals with complex lattices

Weng-Long Liu[1], **Tzong-Jer Yang**[1] **and Ben-Yuan Gu**[2]

[1] Department of Electrophysics, National Chiao Tung University, Hsinchu 30050, Taiwan, Republic of China
[2] Institute of Physics, Academia Sinica, PO Box 603, Beijing 100080, People's Republic of China

Received 20 February 2004
Published 11 June 2004
Online at stacks.iop.org/JPhysCM/16/4557
doi:10.1088/0953-8984/16/25/013

Abstract

Two-dimensional tunable photonic crystals (TPCs) with movable components are proposed, which consist of a circular dielectric rod inserted into a square lattice of square dielectric cylinders in air. The band gap structures of TPCs can be tuned by adjusting the shift of the position of the circular rod in each unit cell. Band gap structures are calculated with the use of the plane-wave expansion method for various structural parameters, such as different filling fractions, ratio of the radius of the circular rod to the side-length of the square cylinder, different shifts or shifting orientations of the circular rod, etc. We find that there is a region of parameters in which the ratio of the gap width to the midgap is insensitive to the shift of the position of the circular dielectric rod. It is anticipated that the proposed TPC may become a favourable candidate of PCs owing to the benefit of facilitating fabrication, allowing a large tolerance.

1. Introduction

During the past decade, novel properties and means of fabricating periodically modulated dielectric structures have attracted much attention. One of the important characteristics of such materials—the so-called photonic crystals (PCs)—is that they exhibit photonic band gaps (PBGs) in which the propagation of electromagnetic (EM) waves in any propagating direction and polarization state is inhibited [1–6]. This feature leads to various peculiar physical phenomena [7] and provides potential applications [8–11].

Most proposed applications of PCs rely on the large PBGs of PCs; therefore, the design and construction of PCs with large PBGs are major goals in the PC field [8–11]. Various methods have been proposed and implemented, for instance, introducing additional scatterers into the unit cell of the prototype lattices to lift the degeneracy of the photonic bands at high symmetric points in the first Brillouin zone (FBZ) [12], rotating the lattices [13], employing

anisotropic dielectric materials [14], rotating the non-circular rods [15–18], modifying the distribution of permittivity in the unit cell [19–21], etc. Other design schemes with the use of various materials and mechanisms have also been developed [22–28].

In view of practical applications, a PC with tunable PBGs (TPBGs) is favourable because of the tunability of the operation frequency in optical or microwave devices; thus, recently, TPCs have received much attention. Various materials have been suggested for the realization of the TPCs, including liquid crystals [29–31], metals and semiconductors [32–35], ferrites [36], piezoelectric materials [37] and other optical materials [38, 39].

Motivated by these works, in this article we propose an alternative scheme of the construction of TPCs. The proposed two-dimensional TPC structure is realized by inserting a movable circular dielectric rod into a square lattice of square dielectric cylinders in air. The PBGs can be tuned by shifting the position of the circular dielectric rod. Indeed, several similar researches have been reported [13, 15–18]. Their studies predominantly focused on the studies of the effects of rotating the 2D lattices or scatterers on PBGs. However, in the present work, we mainly concentrate on the subject of the sensitivity of the ratio $\Delta\omega/\omega_{\mathrm{g}}$ (where $\Delta\omega$ is the width of the complete band gap and ω_{g} is the midgap) to the variations of the structural parameters of system, especially paying attention to the effects of the shift s of the position of the circular dielectric rod. The band structures of the TPCs are calculated with the use of the plane-wave expansion method. Numerical simulations show that there is a range of parameters in which the variations of $\Delta\omega/\omega_{\mathrm{g}}$ are insensitive to the changes of s. Thus, we conclude that the proposed TPCs may become a favourable candidate of PCs owing to the facilitated fabrication with an allowance of large tolerance.

The rest of this paper is organized as follows. Section 2 briefly describes the model structures and the fundamental formulae used in calculations. Section 3 presents the numerical results and the analysis. Finally, section 4 discusses and summarizes the main findings.

2. Structural model and fundamental formulae

The schematic diagram of the proposed TPC structure is displayed in figure 1. The square dielectric cylinders with a side-length of l and dielectric ϵ_{a} are placed in air with $\epsilon_{\mathrm{b}} = 1.0$ at the four corners of a 2D square lattice with a lattice constant a in the xy-plane. Another circular dielectric rod with $\epsilon = \epsilon_{\mathrm{a}}$ and diameter d is inserted into each unit cell, forming composite lattices. We denote $\beta = d/l$ for convenience.

The electromagnetic (EM) fields with the E/H-polarization (in-plane magnetic/electric fields) in the 2D PC are governed by Maxwell's equations:

$$\left\{\nabla \times \frac{1}{\epsilon(\mathbf{r})}\nabla\times\right\}\mathbf{H}(\mathbf{r}) = \frac{\omega^2}{c^2}\mathbf{H}(\mathbf{r}), \tag{1}$$

where $\mathbf{H}(\mathbf{r})$ denotes the magnetic fields, ω the angular frequency, c the speed of light in vacuum, and $\epsilon(\mathbf{r})$ the periodically modulated dielectric function. The magnetic fields and the dielectric function can be expanded in terms of Fourier series as

$$\mathbf{H}(\mathbf{r}) = \sum_{\mathbf{G}}\sum_{\lambda=1}^{2} h_{\mathbf{G},\lambda}\hat{\mathbf{e}}_{\lambda}\mathrm{e}^{\mathrm{i}(\mathbf{k}+\mathbf{G})\cdot\mathbf{r}}, \tag{2}$$

$$\epsilon(\mathbf{r}) = \sum_{\mathbf{G}} \epsilon(\mathbf{G})\mathrm{e}^{\mathrm{i}\mathbf{G}\cdot\mathbf{r}}, \tag{3}$$

where $\mathbf{k}$ is the Bloch wavevector in the FBZ, and $\mathbf{G}$ the 2D reciprocal lattice vector. The polarization unit vectors $\hat{\mathbf{e}}_{\lambda}$ with $\lambda = 1, 2$ are perpendicular to $(\mathbf{k}+\mathbf{G})$, and $h_{\mathbf{G},\lambda}$ is the Fourier expansion component of the magnetic fields. The Fourier coefficient $\epsilon(\mathbf{G})$ is given by

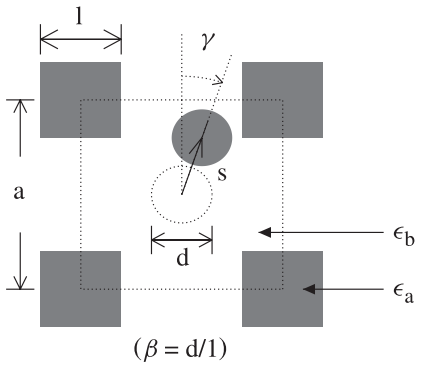

Figure 1. Schematic diagram of proposed tunable photonic crystals. The square dielectric cylinders with a side-length of l and dielectric ϵ_a are placed in air with $\epsilon_b = 1.0$ at the four corners of a 2D square lattice with a lattice constant a in the xy-plane. Another circular dielectric rod with $\epsilon = \epsilon_a$ and diameter d is inserted into each unit cell, forming composite lattices. We denote $\beta = d/l$ for convenience. This dielectric circular rod is movable. We assume that there is a shift $\mathbf{s}$ of the inserted circular rod with respect to the centre of the unit cell, that is $\mathbf{s} = s(\hat{\mathbf{x}} \sin\gamma + \hat{\mathbf{y}} \cos\gamma)$, where γ is the span angle of the displacement vector with respect to the y-axis.

$$\epsilon(\mathbf{G}) = \frac{1}{A_{\text{cell}}} \int_{\text{cell}} \epsilon(\mathbf{r}) \mathrm{e}^{-\mathrm{i}\mathbf{G}\cdot\mathbf{r}} \, \mathrm{d}\mathbf{r}, \tag{4}$$

where the integration is performed over the unit cell. Here, the filling fraction f, which is the ratio of the areas A_{scat} of dielectric scatterers in a unit cell to the area A_{cell} of a unit cell of square lattice, is

$$f = \frac{l^2}{a^2}\left(1 + \frac{\pi\beta^2}{4}\right). \tag{5}$$

For the proposed TPC, $\epsilon(\mathbf{G})$ is evaluated by

$$\epsilon(\mathbf{G}) = \begin{cases} f\epsilon_a + (1-f)\epsilon_b & \text{for } \mathbf{G} = 0, \\ (\epsilon_a - \epsilon_b) S(\mathbf{G}) & \text{for } \mathbf{G} \neq 0. \end{cases} \tag{6}$$

We assume that there is a shift $\mathbf{s}$ of the inserted circular rod with respect to the centre of the unit cell, that is $\mathbf{s} = s(\hat{\mathbf{x}} \sin\gamma + \hat{\mathbf{y}} \cos\gamma)$, where γ is the span angle of the displacement vector with respect to the y-axis. The structural factor $S(\mathbf{G})$ is then given by [40]

$$S(\mathbf{G}) = \mathrm{e}^{-\mathrm{i}\mathbf{G}\cdot(\hat{\mathbf{x}}+\hat{\mathbf{y}})a/2} S_1(\mathbf{G}) + \mathrm{e}^{-\mathrm{i}\mathbf{G}\cdot\mathbf{s}} S_2(\mathbf{G}), \tag{7}$$

where

$$S_1(\mathbf{G}) = \left(\frac{l^2}{a^2}\right) \mathrm{Sinc}\left(\frac{G_x L}{2}\right) \mathrm{Sinc}\left(\frac{G_y L}{2}\right) \tag{8}$$

with $\mathrm{Sinc}(x) = \sin x / x$ and

$$S_2(\mathbf{G}) = \left(\frac{l^2}{a^2}\right) \frac{\pi\beta^2}{2} \frac{J_1(Ga)}{Ga}, \tag{9}$$

where $J_1(x)$ is the Bessel function of the first kind, and $G = |\mathbf{G}|$.

The band structures are then determined from solving the following equation:

$$\sum_{\mathbf{G}'} A(\mathbf{k}+\mathbf{G}, \mathbf{k}+\mathbf{G}') H(\mathbf{G}') = \omega^2 H(\mathbf{G}) \tag{10}$$

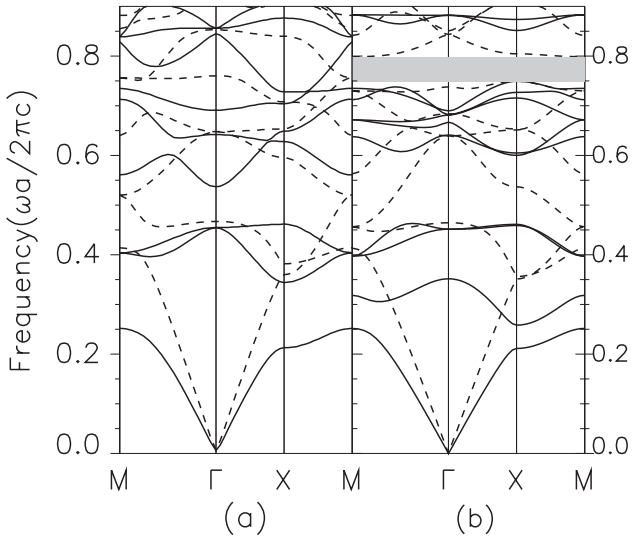

Figure 2. Photonic band structures for two structures: (a) the prototype structure without the inserted circular rod, and (b) a TPC with a movable dielectric circular rod in the interior of the unit cell. The relevant parameters are chosen as $\epsilon_a = \epsilon = 11.4$, appropriate for GaAs material, and $\epsilon_b = 1.0$ in air. (a) $f = 0.217$, $d/l = 0$ and (b) $f = 0.3$, $d/l = 0.7$, $s = 0$. The solid and dashed curves correspond to the E- and H-polarizations, respectively. The shaded area marks the complete gap region.

with

$$A(\mathbf{K}, \mathbf{K}') = \begin{cases} |\mathbf{K}||\mathbf{K}'|\epsilon^{-1}(\mathbf{K} - \mathbf{K}') & \text{for the } E\text{-polarization state,} \\ \mathbf{K} \cdot \mathbf{K}'\epsilon^{-1}(\mathbf{K} - \mathbf{K}') & \text{for the } H\text{-polarization state,} \end{cases} \tag{11}$$

where $\mathbf{K} = \mathbf{k} + \mathbf{G}$, $\mathbf{K}' = \mathbf{k} + \mathbf{G}'$. $\epsilon^{-1}(\mathbf{K} - \mathbf{K}') = \epsilon^{-1}(\mathbf{G} - \mathbf{G}')$ can be computed from solving the following equation:

$$\sum_{\mathbf{G}''} \epsilon^{-1}(\mathbf{G} - \mathbf{G}'')\epsilon(\mathbf{G}'' - \mathbf{G}') = \delta_{\mathbf{G}\mathbf{G}'}. \tag{12}$$

3. Numerical results and analysis

The following parameters are used in the calculations: $\epsilon_a = \epsilon = 11.4$ appropriate for gallium arsenide (GaAs) at wavelength $\lambda \approx 1.5$ μm, and $\epsilon_b = 1.0$ in air. 1521 plane waves in the Fourier expansion are used to calculate the PBGs for the $E(H)$-polarization. First, the PBG structures of the prototype square lattices just with square cylinders are calculated, as shown in figure 2(a), with the filling fraction fixed at $f = 0.217$. The solid (dashed) curves correspond to the $E(H)$-polarization. Hereafter, we always adopt these line styles in the same manner to plot the photonic band structures except when another description is given. It is clearly seen that there are two large PBGs (solid curves) for the E-polarization: $\omega_{g1} = 0.3(2\pi c/a)$ and $\omega_{g2} = 0.5(2\pi c/a)$; however, no PBG survives for the H-polarization. Thus, the complete PBG is now absent in the prototype PC. In contrast, when a circular GaAs rod is introduced into each unit cell, the calculated band structures are as demonstrated in figure 2(b). It is evident that a complete PBG is now generated, as indicated by the grey region. The parameters are $f = 0.3$, $\beta = 0.7$, and $s = 0$. This PBG becomes a complete one when E_9 and H_6 are

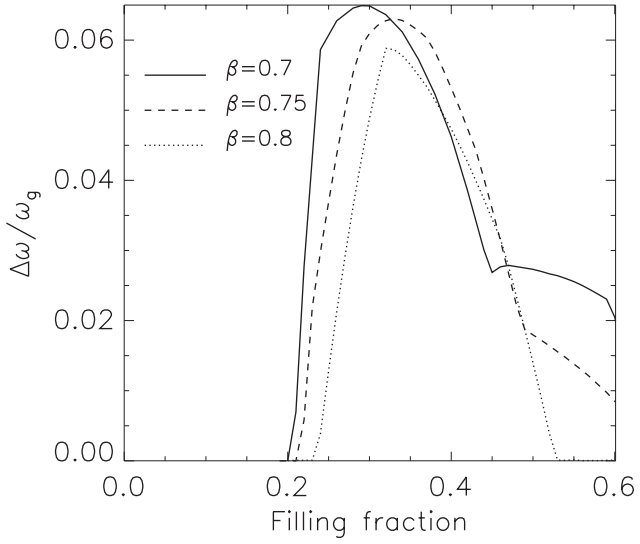

Figure 3. Variations of $\Delta\omega/\omega_g$ with the filling fraction f for different values of β: 0.7 (solid curve), 0.75 (dashed curve) and 0.8 (dotted curve). The other parameters are the same as those in figure 2(b).

overlapped with each other, where E_i (H_i) denotes the band gap appearing between the ith and $(i + 1)$th bands for the $E(H)$-polarization. Notably, introducing an extra circular rod into each unit cell substantially lowers the band frequencies and generates new bands for the E-polarization. These results can be interpreted by considering the effects of scattering and interference of light waves to be significantly modified and enhanced when introducing the extra scatterer into each unit cell [19–21]. For the H-polarization bands, the introduction of the extra scatterer should lead to the lowering of the frequency of the higher index bands, but only a small modification of the profile of the lower index bands.

The effects of the filling fraction f on the dispersion spectrum are revealed by the plot of the dependence of the $\Delta\omega/\omega_g$ as a function of f for different values of β (0.7, 0.75 and 0.8), and fixed $s = 0$, as depicted in figure 3. $\epsilon_a = \epsilon = 11.4$ and $\epsilon_b = 1.0$ are chosen. From $f = (1 + \pi\beta^2/4)(l/a)^2$ and given f as well as β, one can easily evaluate l/a. Notably, the $\Delta\omega/\omega_g$ becomes the largest of all the complete PBGs at a given f and specified β. In the calculations, only the first ten bands are considered for both E- and H-polarizations. Apparently, all of the curves exhibit a Gaussian-like broad bump with a right-hand wing; the non-zero $\Delta\omega/\omega_g$ spans only a finite range, $f = [0.2, 0.6]$. As β is increased, the peak position in the curve is shifted towards the larger f regime, while the right-hand wing falls rapidly. The largest peak value of $\Delta\omega/\omega_g$ is 0.0649, corresponding to $f = 0.29$ and $\beta = 0.7$ (solid curve). As β is altered, this peak value and the profile of $\Delta\omega/\omega_g$ are changed gradually; for instance, $(\Delta\omega/\omega_g)_{max}$ are 0.0649, 0.063 and 0.0589, at $f = 0.29, 0.33, 0.32$ and $\beta = 0.7, 0.75, 0.8$, respectively. The dependence of $(\Delta\omega/\omega_g)$ on f is also calculated at other values of β: the corresponding curves exhibit significantly deformation. The declining trend of the right-hand wing is quite fast and its extension is remarkably shortened as β is increased. This broad bump profile manifests the large freedom in the choice of the structural parameters, which provides the benefit of the facilitated construction of the TPCs with a large allowance of tolerance.

The influences of the shift s of the dielectric circular rod on the PBGs are now investigated. The sample is the same as that in figure 2(b), except that s is changed. Figure 4 depicts the calculated band structures for two values of s: (a) $s = 0.1a$, (b) $s = 0.25a$. The other

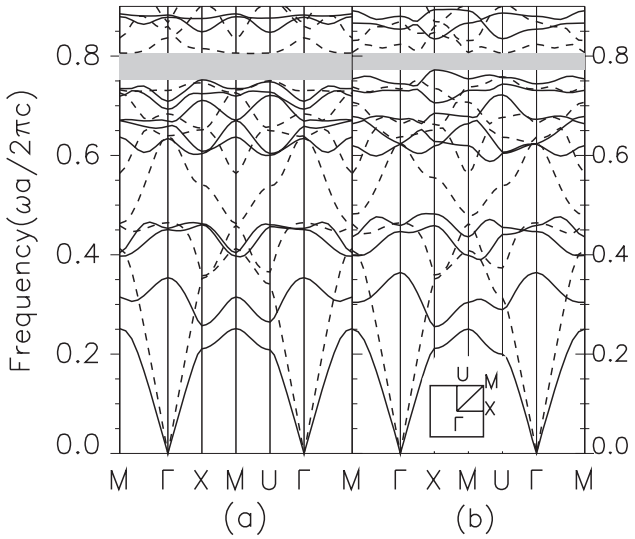

Figure 4. The same as figure 2(b) except for different values of s: (a) $s = 0.1a$ and (b) $s = 0.25a$. The other parameters are $f = 0.3$, $\beta = 0.7$, and $\gamma = 0°$.

parameters are $f = 0.3$, $\beta = 0.7$, $\epsilon_a = \epsilon = 11.4$ and $\epsilon_b = 1.0$, at fixed $\gamma = 0°$. The shift of the inserted circular rod leads to lowering the symmetry of the structures and lifting the degeneracy at the high symmetric points in the FBZ; therefore, the complete PBG can be produced. Figure 4 demonstrates the existence of a complete PBG with $\omega_g = 0.778\,05(2\pi c/a)$ and $\Delta\omega = 0.0509(2\pi c/a)$, which covers the overlapping region of the E_9 and H_7 bands. When s is increased to $0.25a$, the complete gap remains, but the midgap is slightly changed: $\omega_g = 0.787\,95(2\pi c/a)$; however, the gap width is reduced substantially to $\Delta\omega = 0.0311(2\pi c/a)$, as shown in figure 4(b). The increase of s significantly shifts the top of the E_9 band upwards, but the bottom of the H_7 band remains almost unchanged; consequently, the gap is narrowed considerably.

We now study the influences of the direction of the displacement of the inserted dielectric circular rod on $\Delta\omega/\omega_g$. The following parameters are chosen: $f = 0.3$, $\beta = 0.7$; the other parameters are as those in figure 4. The variations of $\Delta\omega/\omega_g$ with s are shown in figure 5 for three different shifting directions of $\gamma = 0°$, 25° and 45°. Notably, for a given γ, the varying region of s is limited, i.e., only from zero to a certain value at which the outermost edge of the internal dielectric circular rod just touches the outermost edge of the square dielectric cylinder at the lattice or the boundary of the unit cell of the lattice. All the curves in figure 5 exhibit a plateau profile at around $\Delta\omega/\omega_g = 0.07$ at the beginning of curves, and then decline monotonically to zero at a certain s, depending on γ. Subsequently, the curves, except for the solid one with $\gamma = 0°$, oscillate with s, as shown in figure 5. Importantly, these plateaus in curves have only a small positive slope near the beginning. This plateau spans a finite region of about $s = [0, 0.1]a$; thus, it can greatly relax the tolerance in the fabrication of TPCs.

The convergence of the calculated results with the increase of the number of plane-waves in the expansion needs to be confirmed with the robustness and reliability of the obtained results.

The variations of $\Delta\omega/\omega_g$ of the complete band gap as a function of the number N of the plane-waves in the expansion are depicted in figure 6. The following parameters are used: $f = 0.3$, $\beta = 0.7$, $s = 0.1\,a$ and $\gamma = 0°$. Clearly, the curve tends to a saturation

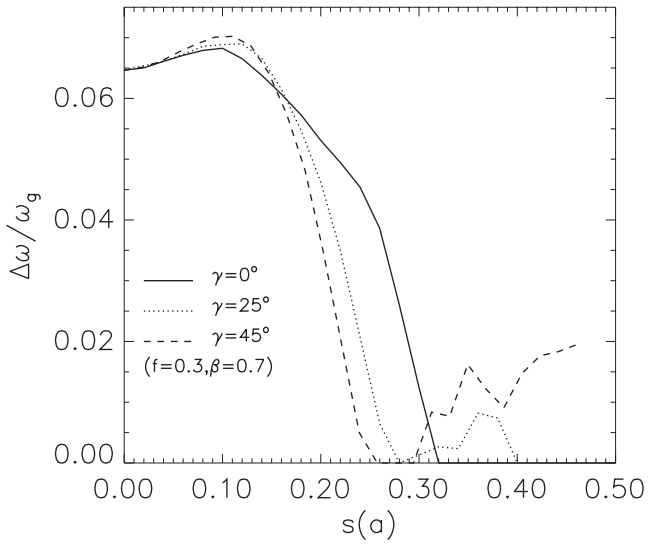

Figure 5. Variations of $\Delta\omega/\omega_g$ with the relative shift s for several shifting directions: $\gamma = 0°$ (solid curve); $\gamma = 25°$ (dotted curve), and $\gamma = 0.45°$ (dashed curve). The other parameters are the same as those in figure 2(b).

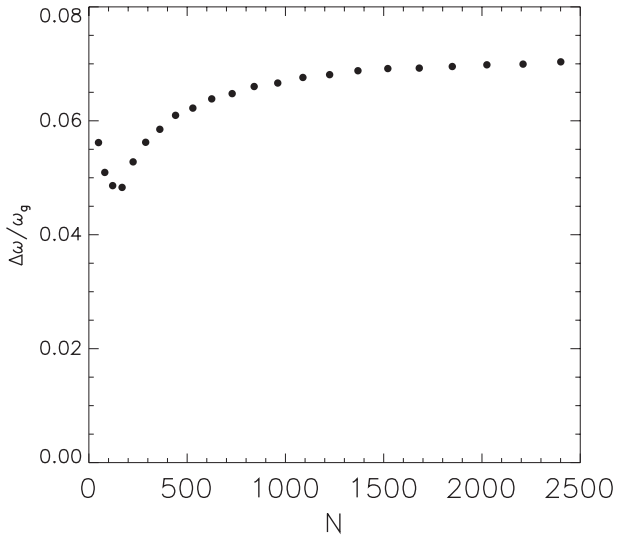

Figure 6. Variations of $\Delta\omega/\omega_g$ of the complete band gap versus the number N of the plane-waves in the expansion. The parameters are $f = 0.3$, $\beta = 0.7$, $s = 0.1\,a$ and $\gamma = 0°$.

value of about 0.068 as N increases. The relative error defined by $[(\Delta\omega/\omega_g)(\text{at } N = 2500) - (\Delta\omega/\omega_g)(\text{at } N = 1521)]/0.5[(\Delta\omega/\omega_g)(\text{at } N = 2500) + (\Delta\omega/\omega_g)(\text{at } N = 1521)]$ is 0.016. In the calculation herein, $N = 1521$ is used. Therefore, these results are reliable.

To confirm the existence of the plateau, we study the $(\Delta\omega/\omega_g)$–s dependence for several N; these are displayed in figure 7. The relative errors defined by $[(\Delta\omega/\omega_g)(\text{at } N = 3249) - (\Delta\omega/\omega_g)(\text{at } N = 1521)]/0.5[(\Delta\omega/\omega_g)(\text{at } N = 3249) + (\Delta\omega/\omega_g)(\text{at } N = 1521)]$ are 0.023,

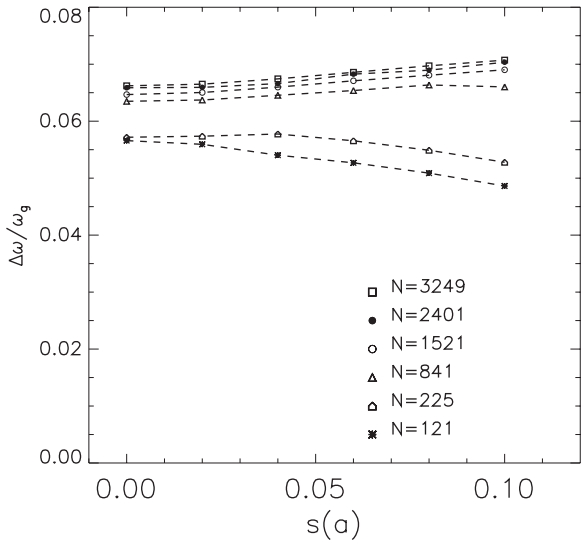

Figure 7. Variations of $\Delta\omega/\omega_g$ of the complete band gap with s as the number N of the plane-waves in the expansion increases for $\gamma = 0°$ with $f = 0.3$, $\beta = 0.7$. The numbers of plane-waves in the expansions for the H-polarization and the E-polarization are the same.

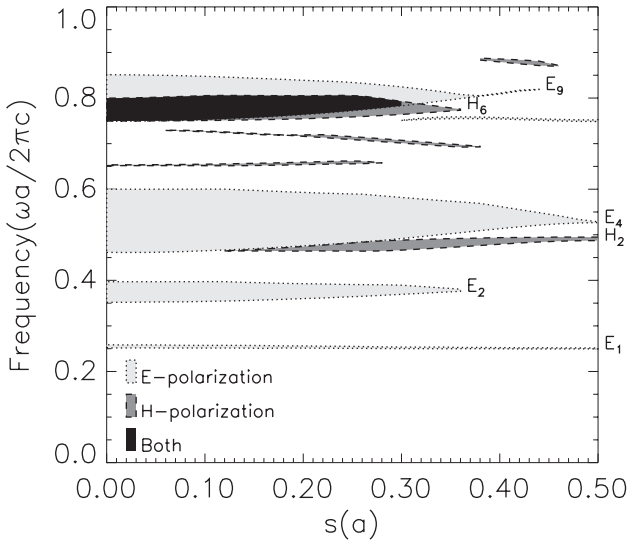

Figure 8. Gap map of the proposed TPC, as the relative shift s varies for both E- and H-polarizations. The parameters are $f = 0.3$, $\beta = 0.7$, and $\gamma = 0°$. The black area marks the regions of the complete band gaps.

0.0221, 0.0217, 0.0219, 0.0239 and 0.0243 for $s = 0.0$, 0.02, 0.04, 0.06, 0.08 and 0.1, respectively. This implies that the existence of the plateau is believable.

An additional plot in figure 8 provides more information on the TPCs. The PBG map as the relative shift s of the inserted rod varies is presented. The parameters are chosen as $f = 0.3$, $\beta = 0.7$ and $\gamma = 0°$. Only the first ten bands are involved in this map for both E- and H-polarizations. Notably, all the gap widths for the E-polarization gradually shrink

as s increases. The E_1 and E_4 band gaps are in the range $s = [0, 0.5]a$, while the gap width of the E_1 band is quite small and almost unobservable. The gaps of the E_2 and E_9 bands span a short region of s less than $0.4a$. For the H-polarization modes, the gap region for the H_2 and H_6 bands covers only a narrow range of s, and the gap width is narrower than that in the E-polarization case. Only one complete PBG appears between H_7 and E_9, and it is marked by the black area in figure 8. It starts near $s = 0$ and ends at about $0.31a$. The complete PBG is centred near $\omega a/2\pi c = 0.775$ with $\Delta\omega/\omega_g = 0.0646$ when $s = 0$.

4. Discussions and summary

Tunable PCs containing a movable dielectric circular rod in each unit cell are proposed. Such TPCs can be fabricated by separately building two 2D PCs; one PC consists of dielectric circular rods located in the interior of a square lattice, and the other PC consists of dielectric square cylinders located at the four corners of a square lattice with the identical lattice constant, a. They are then combined into a final interpenetrating structure. Properly adjusting the position of the dielectric circular rod in the unit cell enables the tunable *complete* PBG generated from the composite structure to be opened and closed. Additionally, when the relative shift s of the circular rod is under $0.1a$, the ratio of the gap-width to the midgap remains almost unchanged or varies only a little. This property provides the large benefit of relaxing the fabrication tolerance of the TPCs. The TPCs can be easily fabricated and operated in the microwave region because a is of the order of microwave wavelengths—several millimetres or centimetres.

In summary, the properties of the proposed TPCs are systematically investigated. When the filling fraction f and the ratio of the diameter of the dielectric circular rod to the side-length of the dielectric square cylinder, $\beta = d/l$, are suitably chosen, a range of relative shift of the circular rod exists in which the gapwidth–midgap ratio $\Delta\omega/\omega_g$ is insensitive to changes of s, regardless of the direction of **s**. Such insensitivity provides large advantage for the practical fabrication of TPCs, allowing large tolerance. The proposed TPCs are anticipated to be encouraged in applications to new microwave devices. Their acoustic counterparts [16] can also be created and used as tunable acoustic crystals.

Acknowledgments

The authors would like to thank the National Science Council of the Republic of China, Taiwan (Contract No. NSC 90-2112-M-009-028) and the Electrophysics Department, National Chiao Tung University, Taiwan, for their support. Dr Young-Chung Hsue and Dr Pi-Gang Luan are appreciated for their useful discussions.

References

[1] Yablonovitch E 1987 *Phys. Rev. Lett.* **58** 2059
[2] John S 1987 *Phys. Rev. Lett.* **58** 2486
[3] Pilhal M and Maradudin A A 1991 *Phys. Rev.* B **44** 8565
[4] Villeneuve P R and Piché M 1992 *Phys. Rev.* B **46** 4973
[5] Kee C S, Kim J E and Park H Y 1997 *Phys. Rev.* B **56** R6291
[6] Agio M and Andreani L C 2000 *Phys. Rev.* B **61** 15519
[7] John S 1997 *Nature* **390** 661
[8] Soukoulis C M (ed) 1993 *Photonic Band Gaps and Localization* (New York: Plenum)
[9] Joannopoulos J D, Meade R D and Winn J N 1995 *Photonic Crystals—Molding the Flow of Light* (Princeton, NJ: Princeton University Press)
[10] Sakoda K 2001 *Optical Properties of Photonic Crystals* (Berlin: Springer)

[11] Yablonovitch E 2001 *Sci. Am.* **285** 34
[12] Anderson C M and Giapis K P 1996 *Phys. Rev. Lett.* **77** 2949
[13] Anderson C M and Giapis K P 1997 *Phys. Rev.* B **56** 7313
[14] Li Z Y, Gu B Y and Yang G Z 1998 *Phys. Rev. Lett.* **81** 2574
Li Z Y, Gu B Y and Yang G Z 1999 *Eur. Phys. J.* B **11** 65
[15] Wang X H, Gu B Y, Li Z Y and Yang G Z 1999 *Phys. Rev.* B **60** 11417
[16] Goffaux C and Vigneron J P 2001 *Phys. Rev.* B **64** 075118
[17] Wang R Z, Wang X H, Gu B Y and Yang G Z 2001 *J. Appl. Phys.* **90** 4307
[18] Susa N 2002 *J. Appl. Phys.* **91** 3501
[19] Meade R D, Rappe A M, Brommer K D and Joannopoulos J D 1993 *J. Opt. Soc. Am.* B **10** 328
[20] Qiu M and He S 2000 *J. Opt. Soc. Am.* B **17** 1027
[21] Zhang X D, Zhang Z Q, Li L M, Jin C, Zhang D, Man B and Cheng B 2000 *Phys. Rev.* B **61** 1892
[22] Sievenpiper D F and Yablonovitch E 1998 *Phys. Rev. Lett.* **80** 2829
[23] Zhang W Y, Lei X Y, Wang Z L, Zheng D G, Tam W Y, Chan C T and Sheng P 2000 *Phys. Rev. Lett.* **84** 2853
[24] Sigalas M M, Soukoulis C M, Biswas R and Ho K M 1997 *Phys. Rev.* B **56** 959
[25] Kee C S, Kim J E and Park H Y 1998 *Phys. Rev.* E **57** 2327
[26] Gates B and Xia Y 2001 *Adv. Mater.* **13** 1605
[27] Bozhevolnyi S I, Erland D J, Leosson K, Skovgaard P M W and Hvam J M 2001 *Phys. Rev. Lett.* **86** 3008
[28] David S, Chelnokov A and Lourtioz J-M 2001 *IEEE J. Quantum Electron.* **37** 1427
[29] Busch K and John S 1999 *Phys. Rev. Lett.* **83** 967
[30] Leonard S W, Mondia J P, van Driel H M, Toader O, John S, Busch K, Birner A, Gosele U and Lehmann V 2000 *Phys. Rev.* B **61** R2389
[31] Ha Y K, Yang Y C, Kim J E, Park H Y, Kee C S, Lim H and Lee J C 2001 *Appl. Phys. Lett.* **79** 15
[32] Halevi P and Ramos-Mendieta F 2000 *Phys. Rev. Lett.* **85** 1875
[33] Moroz A 1999 *Phys. Rev. Lett.* **83** 5274
[34] Kee C S and Lim H 2001 *Phys. Rev.* B **64** R121103
[35] Kee C S, Lim H, Ha Y K, Kim J E and Park H Y 2001 *Phys. Rev.* B **64** 085114
[36] Kee C S, Kim J E, Park H Y, Park I and Lim H 2000 *Phys. Rev.* B **61** 15523
[37] Kim S W and Gopalan V 2001 *Appl. Phys. Lett.* **78** 3015
[38] Kopperschmidt P 2001 *Appl. Phys.* B **73** 717
[39] Gu Z Z, Iyoda T, Fujishima A and Sato O 2001 *Adv. Mater.* B **13** 1295
[40] Luan P G and Ye Z 2001 *Preprint* cond-mat/0105428